Deep Learning-based Lung Nodule Detection: A Review

Feifei Zhou[1, *]

[1] School of Computer Science and Technology, Henan Polytechnic University, Jiaozuo, Henan 454000, PR China

Abstract

CT scan acquisition is fast and cost-effective and has become the main lung imaging tool. However, the increase in large numbers of CT scans has placed a heavy burden on radiologists; therefore, automated lung nodule detection techniques are needed to reduce the workload of radiologists and computer-aided detection systems are proposed for further accurate diagnosis of the condition. This review provides a comprehensive overview of recent automated lung nodule detection techniques and challenges, etc., as well as a detailed overview and discussion of current research gaps, future developments, and research trends. Relevant articles published in databases such as IEEE Xplore, Science Direct, PubMed, and Web of Science cover research algorithms published from 2014 to 2023, mainly discussing deep learning-based techniques. The schemes presented in these articles, the databases used, the experimental results, and the performance of the algorithms are compared and discussed. This work aims to introduce researchers and readers to the latest techniques and their advances in the detection of lung nodules in the last decade, which will help researchers and radiologists to further understand the latest techniques in this field.

*Corresponding author. Email: zff@home.hpu.edu.cn

1. Introduction

Generally, pulmonary nodules are characterized as round opaque, or irregular lung lesions with a diameter of up to 30 mm in the chest[1], and the different types of nodules are shown in **Figure 1**. Of these, nodules with large size (>8 mm diameter), subsolid, acicular, and lobulated features are more likely to be malignant[2, 3]. Studies have shown that the five-year survival rate with lung cancer ranges from 10% to 16%, which can increase to 52% if diagnostic treatment is implemented early in the formation of lung cancer[4].

Current literature states that the most commonly observed nodules range in size from 3 mm to 30 mm[5], with the majority of these being less than 9 mm and considered small nodules, and those less than 3 mm are called micronodules, as defined by the American Thoracic Society. Due to their unique nature, they pose many challenges to the task of lung nodule detection. First, similarity. Micronodules are discontinuous in their location and show diversity in their shapes, leading to blurring of the distinction from normal tissues. Second, less feature information. In the commonly used lung nodule dataset, the samples have low resolution and small labeled areas, which contain less obvious feature information and are susceptible to the interference of noise points. Third, the distribution of positive and negative samples in the dataset is uneven. In most of the datasets used for lung nodule detection, the samples containing small targets are predominant, while the samples with large and medium targets are small. Fourth, 3D characteristics. Nodule detection is a more difficult 3D target detection problem than 2D target detection.

There are several different imaging modalities used to detect lung nodules, such as computed tomography (CT) [6, 7], positron emission tomography (PET) [8, 9], and magnetic resonance imaging (MRI) [10, 11]. The most sensitive imaging modality, As the most sensitive imaging modality, CT is the newest and leading imaging tool used to capture images of the lungs, with strong competitive advantages such as fast acquisition speed, cost-effectiveness, and a wide range of applications. Therefore,

most of the research work in this field has been devoted to the detection of lung nodules on chest CT scans.

However, the large increase in CT scans places a heavy burden on radiologists and is a very tedious and time-consuming task. Therefore, automated lung nodule detection and diagnostic technologies are needed to reduce the workload of radiologists and help them make more accurate diagnoses. These technologies are called computer-aided diagnosis (CAD) systems [12, 13]. In general, CAD systems are divided into two systems: computer-aided detection (CADe) systems and computer-aided diagnosis (CADx) systems. CADe systems focus on the location of suspicious lesions in medical images, while CADx systems are designed to help radiologists determine the type of abnormality. CADe systems focus on the location of suspicious lesions in medical images [14, 15], while CADx systems are designed to help radiologists determine the type and malignancy of the abnormality. This article focuses on the CADe system.
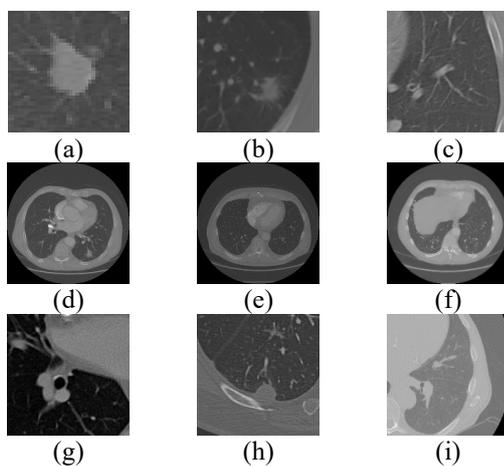
Figure 1. Types of lung nodules. (a) Isolated solid nodule; (b) Frosted glass nodule; (c) Partial solid nodule; (d) Isolated nodule in CT slice; (e) Non-nodule in CT slice; (f) Micro-nodule in CT slice; (g) Nodule in pleural effusion; (h) Subpleural nodule; and (i) Hemivascular nodule.

In the past decade, thanks to the further development of artificial intelligence, research related to pulmonary nodule detection has received more and more attention from researchers. **Figure 2** shows the number of publications in this field from 2014 to 2023, searched using the keywords "pulmonary nodule detection" or "lung nodule detection", which are statistically derived from the core database of the Web of Science.

A significant increase in the number of papers published each year can be seen, reaching a total of 367 in 2022. The total number of papers published in the last decade reached 2,503. This suggests that CADe protocols on lung nodule detection have been a popular research topic over the past 10 years. Although there are many

review papers on CADe protocols, most of these papers do not include CADe protocols that have been studied in recent years; for example, Zhang et al. [16] outlined techniques developed from 2015 to May 2018, which lack a generalized summary of the techniques in recent years and does not do a good job of keeping researchers and radiologists informed of the latest advances.
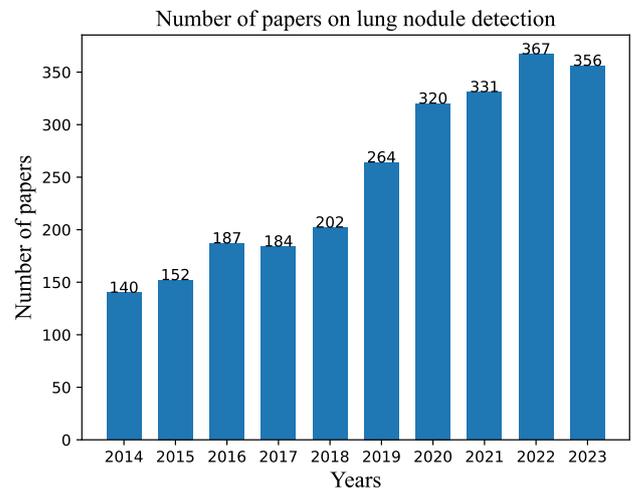
Figure 2. Number of papers on lung nodule detection (2014 to 2023)

This paper not only describes the experimental benchmarks and composition of CADe systems but also compares the key technologies of these systems, emphasizing the various systems developed based on state-of-the-art convolution neural networks (CNNs). In addition, the selected articles are published in databases such as IEEE Xplore, Science Direct, PubMed, and Web of Science. In this paper, the algorithms proposed in these publications, the databases used, the experimental results obtained, and the performance of the algorithms are discussed in comparison. Research trends, current challenges, and future work of the algorithms are also pointed out at the end of the paper. Therefore, this paper is suitable for beginners to learn about lung nodule detection methods, as well as for professional researchers and radiologists to learn more about the latest technology in CADe systems, which is the purpose of this paper.

The architecture of this paper is described according to the following threads. Firstly, it introduces the common datasets and evaluation metrics for lung nodule detection, explains the five important components of lung nodule detection algorithms, and describes their significance, difficulties, and related techniques. Subsequently, the algorithms that have good results on the task of lung nodule detection in recent years are reported, which are useful as a guide for subsequent research. Then, the paper discusses the comparison from several perspectives and points out the research trends, current challenges, and future directions in the development of CADe systems for lung

nodule detection. This review is summarized in the last part.

2. Datasets and evaluation indicators

To develop an effective CADe system, researchers need to focus on datasets and evaluation metrics. A large number of CT scans of the lungs are required to train a detection model for pulmonary nodules, so the acquisition of public datasets is crucial. Second, reliable evaluation metrics are necessary to fairly validate the performance of various algorithms.

2.1. Datasets

Numerous public datasets of lung CT scans have been created to develop, train, and evaluate CADe systems.

1) LIDC-IDRI

The Lung Image Database Consortium and Image Database Resource Initiative (LIDC-IDRI)[17, 18] is the largest publicly available reference database for lung nodules. It contains 1018 CT scans and associated annotated XML files from four experienced radiologists.

2) LUNA16

The Lung Nodule Analysis 2016 (LUNA16)[5] dataset is a subset of LIDC/IDRI. It consists of a total of 888 chest CT scans, based on the fact that each case contains a lesion that has been labeled by at least three of the four medical experts involved in the annotation process. In this dataset, only nodules with a diameter of less than 3 mm were considered positive samples, while all remaining lesions were considered negative samples.

3) ELCAP

The Early Lung Cancer Action Program (ELCAP)[19] is a dataset of 50 low-dose CT cases. The image slice thickness is equal to 1.25 mm, and most of the identified nodules range from 2 to 5 mm in diameter. It is worth mentioning that all labeled lesions in this dataset were nodules and the medical expert did not label any non-nodules.

4) NELSON

The Nederlands Lung Cancer Study (Nederlands-leavens Longkanker screenings Onderzoek, NELSON)[20] included LDCT scans with data from approximately 15,822 participants. The slice thickness for each set of images was 1 mm and the overlap between slices was 0.7 mm. Annotations were generated using LungCare software or manually.

2.2. Evaluation indicators

Validating and measuring the performance of various algorithms requires the use of evaluation metrics. The evaluation metrics commonly used for lung nodule detection are listed below:

1) TPR, FPR, and $Accuracy$

True positive rate (TPR), false positive rate (FPR), and $Accuracy$ are the main evaluation indexes of nodule detection, which need to be calculated using 4 parameters: true positive (TP), true negative (TN), false positive (FP), and false negative (FN). An abnormality in a CT image of the lung is defined as TP or FN if it is a pulmonary nodule, or TN or FP if the abnormality is excluded, i.e., if it is not a pulmonary nodule.

$$\begin{cases} TPR = \dfrac{TP}{TP + FN} \\ FRP = \dfrac{FP}{FP + TN} \\ Accuracy = \dfrac{TP + TN}{TP + TN + FP + FN} \end{cases} \quad (1)$$

2) ROC and FROC

The receiver operating characteristic (ROC) curve represents the relationship between TPR and FPR, with FPR on the X-axis and TPR on the Y-axis. The free-response ROC (FROC) is similar to the ROC curve, except that the number of FPs per scan replaces the FPR.

3) CPM

The competition performance metric (CPM) refers to the average sensitivity at 1/8, 1/4, 1/2, 1, 2, 4, and 8 FPR per scan, defined as the final score of the FROC curve, and has become the evaluation criterion for most competitions in the detection of lung nodules. The CPM is expressed using equation (2), where i denotes the number of FPs per scan at each of the seven predefined FPR levels, and s denotes the sensitivity.

$$CPM = \frac{1}{7}\sum_{i=FPs} s(i), FPs = \left\{\frac{1}{8},\frac{1}{4},\frac{1}{2},1,2,4,8\right\} \quad (2)$$

3. CADe system for lung nodule detection

The CADe system is designed to improve diagnostic accuracy, assist in the early detection of cancer, and reduce the radiologist's examination and evaluation time. As a potential assistant in clinical practice, CADe systems [21, 22] may have different configurations.

In general, CADe consists of five basic steps: data acquisition, preprocessing, lung segmentation, candidate nodule detection, and false positive reduction. These steps are shown in **Figure 3**.
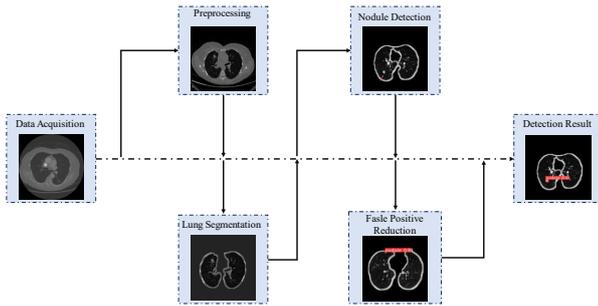
Figure 3. Steps in the CADe system

1) Data acquisition

CT is usually the first choice for early lung nodule screening due to its high sensitivity and relatively low cost compared to other modalities[23].

2) Preprocessing

Generally, to reduce the radiation hazard, radiologists reduce the radiation dose in CT scans, which can degrade the image quality and produce extraneous information such as noise, artifacts[24], etc., and therefore the images need to go through a pre-processing step. The common filters used in this stage of the method are the median filter[25], Gaussian filter[26], point enhancement filter[27], histogram equalization filter[16], and Laplacian of Gaussian (LoG) filter[28].

3) Lung segmentation

To reduce the search space, a lung segmentation operation is required for CT images. The aim is to accurately separate the lung parenchyma from other tissues and organs for better understanding and analysis at subsequent stages to enhance important information[29]. Traditional segmentation algorithms used for lung parenchyma segmentation include thresholding methods, shape-based methods, edge-based methods, morphological methods, etc. In addition, the deep learning-based segmentation algorithms U-Net [30] and FCN [31] are the most widely used.

4) Candidate nodule detection

The purpose of this step is to separate all suspected lung nodules from the volume of interest (e.g., lung parenchyma) as much as possible and to highlight the location of the nodule. This process not only improves CADe's sensitivity in identifying lung nodules, but also ensures that the physician is able to more quickly localize and focus on these suspicious nodules when reviewing diagnostic results.

5) False Positive Reduction

Due to the high sensitivity of the detection algorithms, certain tissues that are morphologically similar to real lung nodules may also be incorrectly labeled as nodules. Therefore, the main task of this step is to accurately differentiate real lung nodules from these pseudonodules, thus screening out real nodules among suspicious ones. By effectively eliminating false nodules, not only can the false-positive rate of the computer-aided detection system (CADe) be significantly reduced and the diagnostic accuracy be improved, but it can also provide physicians with a more reliable and precise diagnostic basis.

4. Detailed description of the algorithm

With the continuous progress of lung nodule detection technology, in recent years, the focus of research has gradually shifted to deep learning-based algorithms, especially CNNs.CNNs, with their excellent feature learning and characterization capabilities, have achieved remarkable results in target detection tasks, which not only promote the rapid development of computer-aided detection systems (CADe), but also establish the mainstream development direction in this field. The CNNs have been used in a variety of applications, including the following.

The CNN structure is shown in **Figure 4**, which usually contains two major parts: the feature extraction layer and the output layer. The feature extraction layer mainly consists of alternating stacks of convolutional and maximum pooling layers, which are responsible for extracting key features from the input image. After feature extraction, the feature map output from the last convolutional layer is usually flattened, i.e., the multi-dimensional feature map is converted into a one-dimensional feature vector. Then the fully connected layer (FC layer) is accessed for higher level feature integration and classification. Finally, the network passes through the SoftMax layer or the output layer, which outputs the category of the image and other relevant information such as target location, confidence level, etc.
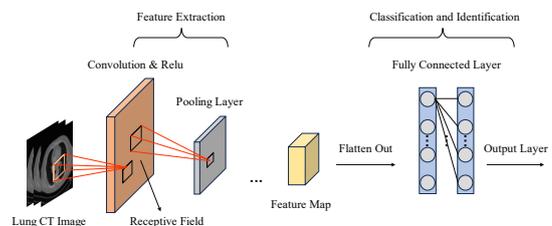
Figure 4. The general structure of CNN

4.1. Detection based on nodule type

The growth morphology and speed of small nodules have an important impact on the formation of lung cancer, therefore, the detection of small nodules is essential.

Zhang Mengyi et al. [32] implemented an improvement on the feature pyramid network (FPN)[33] to address this problem by adding an SE module with a channel attention mechanism to improve detection performance. The optimized 3D FPN architecture was obtained to achieve lung nodule detection. Its effectiveness was validated on the LUNA16 dataset with a CPM of 0.8934. Zheng et al. [34] did the same for small nodule

detection. First, to explore whether MIP-based images can improve the accuracy of nodule detection, four 2D CNNs based on the U-Net architecture and using MIP images with corresponding thickness and axial slices as inputs were applied to detect candidates from the four streams. Subsequently, the results from the four streams are merged into candidate nodules. In the FP removal stage, two VGG-Net-based 3D CNNs are used. The system is trained on the LUNA16 dataset and achieves a sensitivity of 95.36% with 20.4 FPs/scan. However, the algorithm only considered axial slices. Therefore, they proposed another improved architecture in their subsequent work[35]. The designed scheme consists of two stages, namely multiplanar candidate nodule detection and false positive reduction. First, nodule candidates in axial, coronal, and sagittal planes are detected using U-net++. The backbone of U-net++ is the Efficient-Net[36] classification model, pre-trained on ImageNet to efficiently extract a variety of essential features. Predictions from all three planes are merged for higher sensitivity. Subsequently, a multi-scale dense CNN was applied to efficiently remove false-positive nodules. Validation of the LIDC-IDRI dataset showed that the multiplanar approach improved the performance of small nodule detection. A sensitivity of 94.2% was achieved at 1 FPs/scan and 96.0% at 2 FPs/scan.

4.2 Improvements based on traditional detection algorithms

In the target detection task, Faster R-CNN is the classical detection network, which achieves high accuracy detection performance, but still has some shortcomings for the field of lung nodule detection, mainly since the feature maps extracted by backbone are single-layer with small resolution. Therefore, Ding et al. [37] and Su et al. [38] also started from the architecture of Faster R-CNN to develop improved Faster R-CNN for lung nodule detection.

Ding et al. introduced an anti-convolutional structure in Faster R-CNN for detecting nodule candidates from axial slices, and this axial slice composition in 3D helps to reduce the computational effort. Then, the authors utilize 3D DCNN to reduce false positives. The LUNA16 experimental results demonstrate the good performance of the proposed nodule detection method, and the system has an average FROC score of 0.891, which is located in the first place of the challenge. Su et al. concluded that parameter optimization based on Faster R-CNN can theoretically improve the network structure as well as the detection accuracy. Experiments on LIDC-IDRI data showed that the parameters were set to a basic learning rate of 0.001, a step size of 70,000, a decay coefficient of 0.1, a Dropout value of 0.5, and a Batch Size of 64, at which point the highest average accuracy of 83.9% was achieved.

4.3 Based on changes in nodule size and shape

Challenges posed by variations in nodule size and shape are a noteworthy issue, and it is difficult to establish a universal diagnostic criterion because lung nodules are characterized by both size and irregular shape. Based on this, Gu Junhua et al. [39] and Nguyen et al. [40] proposed different ideas.

Inspired by spatial transformation networks[41] and DPM[42, 43], Gu Junhua et al. proposed a deformable convolutional structure to cope with the variable shapes of lung nodules and make the feature extraction process more suitable for the shape of nodules themselves. Another simple but effective strategy is proposed to deal with the variable size of lung nodules. First, the high-level feature maps are deconvoluted and combined with the low-level feature maps to obtain feature maps with rich feature information, and then these feature maps of different levels are used as a prediction layer on which a sliding window is run to generate anchors with different sizes and proportions, and finally, each anchor is classified and bounding-box regressed to ensure that different sizes of lung nodules are detected. The average accuracy of the proposed system can reach 82.7%.

Nguyen et al. argued that most of the designs used for anchors are adopted by default or manually, and these sizes do not match the real lung nodule sizes and shape well, so the authors proposed a Faster R-CNN-based model designed with adaptive anchor sizes. Specifically, the authors generate the adaptive anchor size based on the true nodule size of the dataset by mean-shift (Mean-shift)[44] clustering technique, which produces better performance than the manually-configured anchor method or other clustering-based methods. Subsequently, the authors used ResNet to reduce false positives in the output of the system. Proposed to be trained and tested on the LUNA16 dataset, a high sensitivity of 95.64% was achieved at 1.72 false positives per scan, with a CPM score of 88.2%, which outperforms other recently proposed detection methods.

4.4 Questions based on receptive fields

If the receptive field is too small, only limited contextual information can be utilized to train the network and its recognition ability should not be sufficient to handle large changes in the detection target. If the receptive field is too large, it will result in more redundant information or even noise, reducing the efficiency of the network. Zhang Haowan et al. [45] proposed a framework called LungSeek for nodule detection and classification. For the nodule detection task, they combined selective kernel networks (SK-Net)[46] and 3D ResNet to form a 3D SK-ResNet and applied them to a deep 3D RPN to detect lung nodules. Notably, the SK-Net module can adaptively adjust the receptive field according to the multiple scales of nodules, resulting in better detection of nodules of various sizes. Validated on the LUNA16 dataset, the system achieves

sensitivities of 89.06, 94.53%, and 97.72% for false positives of 1, 2, and 4, respectively.

5. Challenges and prospects

In order to clearly and visually compare and explore the performance of these computer-aided detection (CADe) systems, **Table 1** summarizes some of the key algorithms from recent years and organizes them in chronological order from recent to distant. Each item details the year of publication, author information, dataset used, and a range of key performance metrics including the number of false positives per scan (FPs/scan), sensitivity, accuracy, competitive metrics (CPM), and free response receiver operating characteristic (FROC). With this table, we can comprehensively and systematically evaluate the strengths and weaknesses of each CADe system and provide useful references for researchers and practitioners in related fields.

Table 1. Proposed algorithm

Year	Author	Dataset	Performance
2022	Zhang[47]	LUNA16	0.977 Sen 0.912 CMP
2022	Zhu[48]	LUNA16	0.95 Sen 0.895 CPM
2022	Huang[49]	LUNA16	8 FPs/s, 0.962 Sen CPM 0.905
2022	Zhang[50]	LUNA16	0.927 CPM
2022	Zhang[45]	LUNA16	1 FPs/s, 0.891 Sen 2 FPs/s, 0.945 Sen 4 FPs/s, 0.977 Sen
2022	Luo[51]	LUNA16	7 FPs/s, 0.892 Sen
2021	Nguyen[40]	LUNA16	1 FPs/s, 0.956 Sen 0.882 CPM
2021	Yuan[52]	LUNA16	4 FP/s 0.952 Sen 8 FP/s 0.962 Sen 0.881 CPM
2021	Lin[53]	LUNA16	0.739 Acc
2021	Lai[54]	LUNA16	0.864 Sen 0.950 Acc
2021	Su[38]	LIDC/IDRI	0.839 Acc
2021	Zhang[21]	LUNA16	0.893 CPM
2021	Mei[55]	PN9	0.645 FROM
2021	Peng[56]	LUNA16	0.923Sen
2020	Zheng[35]	LIDC/IDRI	1 FPs/s, 0.942 Sen 2 FPs/s, 0.960 Sen
2020	Xiao[57]	LUNA16	0.991 Sen

5.1. Comparison

This subsection will compare the selected works from different perspectives, categorized as follows:

1) Datasets

As publicly available datasets, LIDC/IDRI and LUNA16 are applied in most of the people's studies, reaching 92.5% of these selected works. New datasets have also been proposed, such as the PN9 dataset by Mei et al. [55], to solve the problem of limited samples and categories in these publicly available datasets.

2) 2D/3D Processing

For the early developed systems, since 3D-based algorithms are not mature, most of them use 2D-based processing, and they do it by inputting the slices into the system one by one. Compared with the 3D approach, although the amount of computation is reduced, the correlation between slices is ignored, while the 3D nature of CT scans is not noticed. Considering these factors, in recent years, 2D-3D or 3D-based input approaches have been adopted by more and more CADe schemes, such as Zhang Guanglu et al. [47] and Zhu Xiaoyu et al. [48].

3) Balance between sensitivity and false positives

Generally speaking, to make the developed CADe system detect as many suspicious nodules as possible, the detector threshold is set very low, but at the same time, some normal tissues such as blood vessels are also determined as suspicious nodules, resulting in a high number of false positives. For example, in the nodule size adaptive depth model proposed by Wang et al. [58], when the sensitivity reaches 96.8%, 60 false positives appear in each scan, and when it is reduced to 15 false positives, the sensitivity will also be reduced to 90%. It is therefore difficult to strike a good balance between the two. However, some researchers have broken this limitation, for

example, Nguyen et al. [40] achieved a low false positive rate of 1.72 FPs/s with a sensitivity of 95.64%, which may be due to their proposed Mean-shift technique.

4) Types of nodules

Most current protocols aim to detect a wider range of nodules without regard to the type of nodule, and some focus more on detecting specific nodules. For example, Gu Yu et al. [59] and Zhang Mengyi et al. [32] focus on the detection of small nodules, Monkam et al. [60] focus on the detection of micronodules, while Li et al. [61] address the identification of three types of nodules. These detection schemes dedicated to specific domains or specific nodules do not achieve high sensitivity and accuracy and have low performance compared to other schemes.

5) Detection method

Lung nodules appear as circular or elliptical tissue lesions, and the use of traditional bounding boxes does not match their representational properties. Luo et al. [51] replaced the commonly used bounding box with a bounding sphere in order to match the annotation of nodules in clinical practice, in order to represent nodules with center of mass, radius, and local offsets in 3D space. A compatible sphere-based loss function (L_{SIoU++}, where SIoU is fully referred to as Sphere Intersection-over-Union) is introduced to stably and efficiently train lung nodule detection networks.

5.2. Discussion

From the above survey of CADe systems, it is clear that significant progress has been made in automated lung nodule detection systems. In this subsection, research trends, challenges, and future directions will be discussed.

1) Research Trends

Deep learning and especially CNN-based schemes have shown good performance and are the main methods for lung nodule detection and classification. As in Section 1, this paper searches the Web of Science core database for literature in the last decade and uses the keywords "pulmonary nodule detection" or "lung nodule detection" with "CNN". "and "CNN" as logical expressions to get the statistical results, as shown in **Figure 5**.

The statistics in the direction of lung nodule detection show that CNN-based solutions are on the rise in general. Among the CNN-based papers published in the decade 2014-2023, the number of publications in 2020 was 83, accounting for 21%. The total number of published papers has reached 393 in the last decade. This shows that CNN-based schemes are the research trend for lung nodule detection.
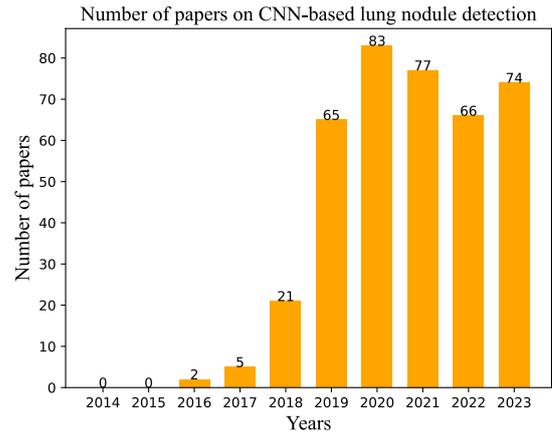
Figure 5. Number of papers on CNN-based lung nodule detection (2014 to 2023)

2) Challenges

1. Insufficient medical datasets

It is worth noting that the large number of labeled medical images is a key factor for the great success of deep learning techniques. However, there are many difficulties such as labeled data being too cumbersome and time-consuming, privacy and ethical requirements, etc., which cause collecting such medical datasets to remain challenging.

2. Complexity of model architecture

Typically, CNN-based detection systems achieve better performance by deepening the depth of the network, but as the depth of the network increases, the performance improvement can be minimal, while introducing a new problem of a slow training process. In addition, the complexity of the model architecture can make it difficult to deploy to servers or cell phones, resulting in limited application of the model.

3. Poor interpretability of test results

Most of the currently developed systems do not provide clinically relevant interpretations. However, the interpretability of the detection system not only allows radiologists to understand how the predictions are generated but also allows radiologists to clarify the reasons behind the CADe system's predictions when they are different from the physician's assessment, to eliminate doubts and concerns.

4. Detection of micronodules

Micronodules <3mm in diameter are too difficult to detect compared to other common nodules, and few studies have been done specifically in this area.

3) Future directions

To improve the performance of the CADe system and make a positive contribution to the lung cancer detection task, this paper proposes the following points in the future optimization direction to address the problems mentioned above:

1. To alleviate the problem of insufficient medical datasets, data enhancement strategies can be applied. In

addition, a generative adversarial network (GAN)[62] can be used to get new images. Semi-supervised or unsupervised as well as self-supervised algorithms are most appropriate when there are CT images with missing labels. Of course, it is also good to use migration learning algorithms, by pre-training 3D CNNs on other large-scale datasets and then applying them to the lung nodule detection task.

2. Lightweight development is necessary to address the complexity of the network architecture. The main measures are "network pruning", "quantization" and "knowledge distillation". Deeply separable convolution instead of normal convolution is also a measure to realize lightweight CNN. 3.

3. For the poor interpretability of the model results, a system can be developed to make the detection process open and transparent, rather than just giving the results, so that radiologists can understand the exact process of detecting lung nodules. The TIDE[63] tool can also be used to analyze the causes of errors and the extent to which these errors affect the performance of the model. In addition, Grad-CAM[64] can be used to generate heat maps for visualization and analysis, showing the model's areas of interest and enhancing the interpretability of its decision-making process.

4. to improve the detection of micronodules, this can be achieved by introducing relevant techniques specialized for small targets. For example, the detection of small targets can be realized through multi-scale feature extraction and inverse convolution operations. The mechanism of the adaptive receptive field can also be applied to the detection of small targets.

References

[1] D. M. Hansell, A. A. Bankier, H. Macmahon, T. C. Mcloud, N. L. Müller, and J. Remy, "Fleischner Society: glossary of terms for thoracic imaging," Radiology, vol. 246, no. 3, pp. 697-722, 2008.

[2] A. Snoeckx et al., "Evaluation of the solitary pulmonary nodule: size matters, but do not ignore the power of morphology," Insights Into Imaging, 2018.

[3] Q. Zhou et al., "China National Guideline of Classification, Diagnosis and Treatment for Lung Nodules (2016 Version)," Zhongguo fei ai za zhi = Chinese journal of lung cancer, vol. 19, no. 12, pp. 793-798, 2016.

[4] C. I. Henschke et al., "Early Lung Cancer Action Project: overall design and findings from baseline screening," vol. 354, no. 9173, pp. 0-105, 1999.

[5] A. A. A. Setio et al., "Validation, comparison, and combination of algorithms for automatic detection of pulmonary nodules in computed tomography images: The LUNA16 challenge," Elsevier, 2017.

[6] S.-H. Wang and S. Fernandes, "AVNC: Attention-based VGG-style network for COVID-19 diagnosis by CBAM," IEEE Sens. J., vol. 22, no. 18, pp. 17431 - 17438, 2022.

[7] S.-H. Wang, "Diagnosis of COVID-19 by Wavelet Renyi Entropy and Three-Segment Biogeography-Based Optimization," International Journal of Computational Intelligence Systems, vol. 13, no. 1, pp. 1332-1344, 2020.

[8] S. W. Kang, S. Jeon, Y. G. Lee, and B. S. Ye, "Dopamine transporter positron emission tomography in patients with Alzheimer's disease with Lewy body disease features," Neurobiology of Aging, vol. 134, pp. 57-65, Feb 2024.

[9] A. Sakai et al., "13N-ammonia positron emission tomography for diagnosis and monitoring of ischemia without obstructive coronary artery disease," International journal of cardiology, vol. 395, p. 131392, 2024 Jan 15 (Epub 2023 Sep 2024.

[10] S. Wang, "Magnetic resonance brain classification by a novel binary particle swarm optimization with mutation and time-varying acceleration coefficients," (in English), Biomedical Engineering-Biomedizinische Technik, Article vol. 61, no. 4, pp. 431-441, Aug 2016.

[11] S.-H. Wang, "Unilateral sensorineural hearing loss identification based on double-density dual-tree complex wavelet transform and multinomial logistic regression," Integrated Computer-Aided Engineering, vol. 26, pp. 411-426, 2019.

[12] Y. Zhang, "Pathological brain detection in MRI scanning by wavelet packet Tsallis entropy and fuzzy support vector machine," SpringerPlus, vol. 4, no. 1, 2015, Art no. 716.

[13] Y. Zhang, "Pathological brain detection in MRI scanning via Hu moment invariants and machine learning," Journal of Experimental & Theoretical Artificial Intelligence, vol. 29, no. 2, pp. 299-312, 2017.

[14] Y.-D. Zhang, "Computer-aided diagnosis of abnormal breasts in mammogram images by weighted-type fractional Fourier transform," (in English), Advances in Mechanical Engineering, Article vol. 8, no. 2, Feb 2016, Art no. 11.

[15] S. Wang, "Pathological Brain Detection by a Novel Image Feature—Fractional Fourier Entropy," Entropy, vol. 17, no. 12, pp. 8278-8296, 2015.

[16] G. Zhang et al., "Automatic nodule detection for lung cancer in CT images: A review," Computers in Biology and Medicine, vol. 103, 2018.

[17] S. G. Armato et al., "The Lung Image Database Consortium (LIDC) and Image Database Resource Initiative (IDRI): a completed reference database of lung nodules on CT scans," Academic Radiology, vol. 14, no. 12, pp. 1455-1463, 2007.

[18] Y. H. Lin, "Data Analysis of the Lung Imaging Database Consortium and Image Database Resource Initiative," Academic radiology, vol. 22, no. 4, 2015.

[19] C. I. Henschke et al., "Early lung cancer action project: a summary of the findings on baseline screening," (in eng), The oncologist, vol. 6, no. 2, pp. 147-52, 2001.

[20] Y. Ru Zhao, X. Xie, H. J. de Koning, W. P. Mali, R. Vliegenthart, and M. Oudkerk, "NELSON lung cancer screening study," (in eng), Cancer imaging : the official publication of the International Cancer Imaging Society, vol. 11 Spec No A, no. 1a, pp. S79-84, Oct 3 2011.

[21] Y. D. Zhang, "Fractal Dimension Estimation for Developing Pathological Brain Detection System Based on Minkowski-Bouligand Method," IEEE Access, vol. 4, pp. 5937-5947, 2016.

[22] Y. Zhang, "Image processing methods to elucidate spatial characteristics of retinal microglia after optic nerve transection," Scientific Reports, vol. 6, no. 1, p. 21816, 2016/02/18 2016.

[23] Ezhil, E., Nithila, S. S., and Kumar, "Segmentation of lung nodule in CT data using active contour model and Fuzzy C-mean clustering," Alexandria Engineering Journal, vol. 55, no. 3, pp. 2583-2588, 2016.

[24] X. Li, B. Li, F. Liu, H. Yin, and F. Zhou, "Segmentation of Pulmonary Nodules Using a GMM Fuzzy C-means Algorithm," IEEE Access, vol. PP, no. 99, pp. 1-1, 2020.

[25] J. John and M. G. Mini, "Multilevel Thresholding Based Segmentation and Feature Extraction for Pulmonary Nodule Detection," Procedia Technology, vol. 24, pp. 957-963, 2016.

[26] R. Roy, P. Banerjee, and A. S. Chowdhury, "A Level Set Based Unified Framework for Pulmonary Nodule Segmentation," Signal Processing Letters, IEEE, vol. PP, no. 99, pp. 1-1, 2020.

[27] W. Choi and T.-S. Choi, "Automated pulmonary nodule detection based on three-dimensional shape-based feature descriptor," Computer methods and programs in biomedicine, vol. 113 1, pp. 37-54, 2014.

[28] Javaid et al., "A novel approach to CAD system for the detection of lung nodules in CT images," Computer Methods & Programs in Biomedicine, vol. 135, no. C, pp. 125-139, 2016.

[29] A. El-Baz et al., "Computer-Aided Diagnosis Systems for Lung Cancer: Challenges and Methodologies," International Journal of Biomedical Imaging,2013,(2013-1-29), vol. 2013, p. 942353, 2013.

[30] O. Ronneberger, P. Fischer, and T. Brox, "U-Net: Convolutional Networks for Biomedical Image Segmentation," Springer International Publishing, 2015.

[31] Long, Jonathan, Shelhamer, Evan, Darrell, and Trevor, "Fully Convolutional Networks for Semantic Segmentation," IEEE Transactions on Pattern Analysis & Machine Intelligence, 2017.

[32] M. Zhang, Z. Kong, W. Zhu, F. Yan, and C. Xie, "Pulmonary nodule detection based on 3D feature pyramid network with incorporated squeeze ˋnd ℯxcitation ˋttention mechanism," Concurrency and Computation Practice and Experience, 2021.

[33] T. Y. Lin, P. Dollar, R. Girshick, K. He, B. Hariharan, and S. Belongie, "Feature Pyramid Networks for Object Detection," IEEE Computer Society, 2017.

[34] S. Zheng, J. Guo, X. Cui, R. N. J. Veldhuis, M. Oudkerk, and P. M. A. Van Ooijen, "Automatic Pulmonary Nodule Detection in CT Scans Using Convolutional Neural Networks Based on Maximum Intensity Projection," IEEE Transactions on Medical Imaging, 2019.

[35] S. Zheng et al., "Deep convolutional neural networks for multiplanar lung nodule detection: Improvement in small nodule identification," (in eng), Medical physics, vol. 48, no. 2, pp. 733-744, Feb 2021.

[36] M. Tan and Q. V. Le, "EfficientNet: Rethinking Model Scaling for Convolutional Neural Networks," 2019.

[37] J. Ding, A. Li, Z. Hu, and L. Wang, "Accurate Pulmonary Nodule Detection in Computed Tomography Images Using Deep Convolutional Neural Networks," in Springer, Cham, 2017.

[38] Y. Su, D. Li, and X. Chen, "Lung Nodule Detection based on Faster R-CNN Framework," Computer Methods and Programs in Biomedicine, vol. 200, no. 1, p. 105866, 2020.

[39] J. Gu, Z. Tian, and Y. Qi, "Pulmonary nodules detection based on deformable convolution," IEEE Access, vol. PP, no. 99, pp. 1-1, 2020.

[40] C. C. Nguyen, G. S. Tran, V. T. Nguyen, J. C. Burie, and T. P. Nghiem, "Pulmonary Nodule Detection Based on Faster R-CNN With Adaptive Anchor Box," IEEE Access, vol. 9, pp. 154740-154751, 2021.

[41] M. Jaderberg, K. Simonyan, A. Zisserman, and K. Kavukcuoglu, "Spatial Transformer Networks," MIT Press, 2015.

[42] J. Dai et al., "Deformable Convolutional Networks," IEEE, 2017.

[43] Forsyth and David, "Object Detection with Discriminatively Trained Part-Based Models," Computer, 2014.

[44] D. Comaniciu and P. Meer, "Mean shift: a robust approach toward feature space analysis," IEEE Transactions on Pattern Analysis and Machine Intelligence, vol. 24, no. 5, pp. 603-619, 2002.

[45] H. Zhang and H. Zhang, "LungSeek: 3D Selective Kernel residual network for pulmonary nodule diagnosis," (in eng), The Visual computer, vol. 39, no. 2, pp. 679-692, 2023.

[46] X. Li, W. Wang, X. Hu, and J. Yang, "Selective Kernel Networks," in 2019 IEEE/CVF Conference on Computer Vision and Pattern Recognition (CVPR), 2019, pp. 510-519.

[47] G. Zhang, H. Zhang, Y. Yao, and Q. Shen, "Attention-Guided Feature Extraction and Multiscale Feature Fusion 3D ResNet for Automated Pulmonary Nodule Detection," IEEE Access, vol. 10, pp. 61530-61543, 2022.

[48] X. Zhu, X. Wang, Y. Shi, S. Ren, and W. Wang, "Channel-Wise Attention Mechanism in the 3D Convolutional Network for Lung Nodule Detection," Electronics, vol. 11, no. 10, p. 1600, 2022.

[49] Y. S. Huang, P. R. Chou, H. M. Chen, Y. C. Chang, and R. F. Chang, "One-stage pulmonary nodule detection using 3-D DCNN with feature fusion and attention mechanism in CT image," Computer Methods and Programs in Biomedicine, vol. 220, pp. 106786-, 2022.

[50] H. Zhang, Y. Peng, and Y. Guo, "Pulmonary nodules detection based on multi-scale attention networks," (in eng), Scientific reports, vol. 12, no. 1, p. 1466, Jan 27 2022.

[51] X. Luo et al., "SCPM-Net: An anchor-free 3D lung nodule detection network using sphere representation and center points matching," Med Image Anal, 2022.

[52] H. Yuan, Z. Fan, Y. Wu, and J. Cheng, "An efficient multi-path 3D convolutional neural network for false-positive reduction of pulmonary nodule detection," International journal of computer assisted radiology and surgery, vol. 16, no. 12, pp. 2269-2277.

[53] L. Haibo, T. Shanli, S. Shuang, and L. Haoran, "An improved yolov3 algorithm for pulmonary nodule detection," in 2021 IEEE 4th Advanced Information Management, Communicates, Electronic and Automation Control Conference (IMCEC), 2021, vol. 4, pp. 1068-1072.

[54] K. Lai, T. Nguyen, and T. Le, "Detection of Lung Nodules on CT Images based on the Convolutional Neural Network with Attention Mechanism," Annals of Emerging Technologies in Computing, vol. 5, pp. 78-89, 04/01 2021.

[55] J. Mei, M. M. Cheng, G. Xu, L. R. Wan, and H. Zhang, "SANet: A Slice-Aware Network for Pulmonary Nodule Detection," IEEE Transactions on Pattern Analysis and Machine Intelligence, vol. 44, no. 8, pp. 4374-4387, 2022.

[56] H. Peng, H. Sun, and Y. Guo, "3D multi-scale deep convolutional neural networks for pulmonary nodule detection," (in eng), PloS one, vol. 16, no. 1, p. e0244406, 2021.

[57] Z. Xiao, B. Liu, L. Geng, F. Zhang, and Y. Liu, "Segmentation of Lung Nodules Using Improved 3D-UNet Neural Network," Symmetry, vol. 12, no. 11, p. 1787, 2020.

[58] J. Wang et al., "Pulmonary Nodule Detection in Volumetric Chest CT Scans Using CNNs-based Nodule-Size-Adaptive Detection and Classification," IEEE Access, pp. 1-1, 2019.

[59] Y. Gu et al., "Automatic lung nodule detection using a 3D deep convolutional neural network combined with a multi-scale prediction strategy in chest CTs," Computers in Biology and Medicine, vol. 103, 2018.

[60] P. Monkam et al., "Ensemble Learning of Multiple-View 3D-CNNs Model for Micro-Nodules Identification in CT Images," IEEE Access, vol. 7, pp. 5564-5576, 2019.

[61] W. Li, P. Cao, D. Zhao, and J. Wang, "Pulmonary Nodule Classification with Deep Convolutional Neural Networks on Computed Tomography Images," (in eng), Computational and mathematical methods in medicine, vol. 2016, p. 6215085, 2016.

[62] M. Krichen, "Generative Adversarial Networks," in 2023 14th International Conference on Computing Communication and Networking Technologies (ICCCNT), 2023, pp. 1-7.

[63] D. Bolya, S. Foley, J. Hays, and J. Hoffman, "TIDE: A General Toolbox for Identifying Object Detection Errors," in Computer Vision – ECCV 2020, Cham, 2020: Springer International Publishing, pp. 558-573.

[64] R. R. Selvaraju, M. Cogswell, A. Das, R. Vedantam, D. Parikh, and D. Batra, "Grad-CAM: Visual Explanations from Deep Networks via Gradient-Based Localization," in IEEE International Conference on Computer Vision, 2017.